Hindawi
Journal of Nanomaterials
Volume 2022, Article ID 1107081, 12 pages
https://doi.org/10.1155/2022/1107081

Research Article

Ultrasensitive Detection of Lysozyme upon Conformational Change of DNA Duplex

Phuoc Long Truong,[1,2] **Nguyen Thi Thu Thao**,[1,2] **Huynh Thi Le Huyen**,[1,2] **and Thi Hiep Nguyen**[1,2]

[1]*School of Biomedical Engineering, International University, Ho Chi Minh City 700000, Vietnam*
[2]*Vietnam National University, Ho Chi Minh City 700000, Vietnam*

Correspondence should be addressed to Phuoc Long Truong; tplong@hcmiu.edu.vn

Received 2 May 2022; Accepted 16 August 2022; Published 26 August 2022

Academic Editor: Dong Kee Yi

We report a simple, cost-effective, and ultrasensitive approach for colorimetric detection of lysozyme based on target-induced conformational change of DNA duplex. The detection method utilizes the interaction between DNA aptamer and its target leading to the dissociation of DNA aptamer from the DNA duplex and forms a structured complex. The complementary DNA that detached from the DNA duplex adsorbed on the AuNPs surface protects the nanoparticles against salt-induced aggregation, resulting in maintaining the red dispersed state of AuNPs. Such an approach allowed the femtomolar detection of lysozyme with a wide linear scale ranging from 0.1 to 200 pM by simple spectroscopic analysis with detection time of ~40 min. In case of naked eye detection, the detection limit of nanoaptasensor corresponds to ~0.5 pM. The nanoaptasensor demonstrated high specificity with regard to lysozyme in the presence of a variety of nonspecific proteins. In case of lysozyme detection in simulated saliva samples, the average recoveries were in the range of 90.47 to 105.90%, with the relative standard deviations (RSD) of 3.45-4.89% that suggests a good reproducibility. The results clearly indicated the reliability and applicability of the proposed assay for the simple and rapid detection of lysozyme in real samples. Compared with existing diagnostic assays, the proposed nanoaptasensor showed many advantages regarding simplicity, versatility, cost, and time for analysis. This approach demonstrated a great potential for ultrasensitive and on-site analysis of a wide range of protein biomarkers using plasmonic nanoparticles.

1. Introduction

Disease identification at an early stage and improved imaging of interior body structure, as well as simplicity of diagnostic processes, have been established with the assistance of a modern and promising field called nanotechnology, which has been developed quickly during recent years [1]. Metallic nanoparticles for biosensors are one of the most fascinating use of nanomaterials in medicine that is currently being researched with straightforward, easy, and cost-effective preparation [2, 3]. Among nanoparticles, noble metallic nanoparticles take great attention owing to their strong surface plasmon resonance, high extinction coefficients, and their nanoscale that are comparable in size to biomolecules [4–6]. Moreover, metallic nanoparticles with very small sensing volume could be utilized as nanoprobes for detection of biological interactions occurred at molecular level [7, 8]. The unique properties of noble nanoparticles make them ideal platform for development of colorimetric assays to detect analytes with low cost [3]. It was proved that the miniaturization of biosensors at the nanoscale led to enhancement of the analytical performances [8–10]. The colorimetric assays based on metallic nanoparticles have proved to be very useful for fast, on-site analysis of various analytes because of their excellent analytical performances such as low-cost, simplicity, ultrahigh sensitivity, and specificity with a minimal volume of reagents [11–13]. The typical sensing mechanism employs the resonance peak shift in the visible range owing to the nanoparticle aggregation that induced by analytes via the various types of interactions [3, 14, 15]. As nanoparticle based colorimetric biosensors, gold nanoparticles (AuNPs) are the most researched and widely used metallic nanoparticles for bio-sensing due to distinct physical and chemical characteristics. The alteration in size, shape, surface characteristics, and aggregation state all affect their distinct optical and electrical properties [16–18]. When the nanoparticle-based biosensors attach to the target, the nanoparticles' characteristics are altered [3, 15]. The electrochemical and optical signals related to the changes in target concentration can be used in detecting the presence as well as the quantity of the biomolecules. This is an important premise to develop an easy, rapid, and cost-effective method of diagnosing protein biomarkers, easing the need of method for early detection of diseases.

In recent years, nanotechnology that applies DNA is appearing more and more in the field of biomedical science and engineering. Researchers found that decorating metallic nanoparticles with DNA is an exciting alternative approach in design and development of biosensors [19, 20]. In case of AuNPs, they are commonly functionalized with thiolated DNA. However, the conjugation process that is labor-intensive usually leads to a decrease in the concentration of AuNPs, and the amount of DNA on the nanoparticle surface also needs to optimize before biosensing applications [21, 22]. Lately, the electrostatic interaction between AuNPs and DNA has been utilized for biosensing applications. AuNPs can be capped with DNA in a short time at neutral pH, and this leads to change the surface properties of the nanoparticles. Recent studies have shown that single-stranded DNA (ssDNA) and double-stranded DNA (dsDNA) have different electrostatic properties due to their quadratic structure of DNA. The electrostatic interaction between the positive charge of ssDNA and the negative charge of AuNPs results in absorption of ssDNA on the nanoparticles surface. This adsorption stabilizes the nanoparticle against aggregation via electrostatic repulsion. However, the same mechanism does not work with dsDNA because dsDNA has a stable double-helix geometry which exhibits a negatively charged phosphate backbone [23, 24]. Furthermore, the color of colloidal gold is mainly affected by the *resonance phenomenon of free electrons in the nanoparticles*, and this resonance is strongly influenced by the nanoparticle aggregation [25]. Therefore, the electrostatic difference between ssDNA and dsDNA can be exploited for the development of a nanoparticle-based simple colorimetric assay.

Lysozyme, an antimicrobial protein, was commonly found in various species such as virus, bacteria, fungi, and mammalian tissues and particularly found in abundance in tears, saliva, and mucous. Submucosal glands, neutrophils, and macrophages all produce lysozyme [26, 27]. Normally, it is distributed in secretions and human body tissues at very low concentrations. However, the unusually high increased levels of lysozyme in cells, serum, plasma, and urine are associated with many diseases such as cancers, leukemia, Alzheimer's disease, HIV, meningitis, renal diseases, rheumatoid arthritis, atherosclerosis, and inflammation [27–29]. Lysozyme with its crucial function in the human immune system has been found to be particularly significant as a biomarker for diagnosis of bacterial infections and chronic diseases such as bronchopulmonary dysplasia [30]. Moreover, the simplicity and its small size make it an excellent model for the development of novel diagnostic methods in detection of protein biomarkers. The qualitative and quantitative analysis of the lysozyme can be a helpful index in detecting and monitoring in the progression for several diseases [27, 28, 30]. Currently, the available analytical methods for detection of lysozyme are the high-performance liquid chromatography (HPLC) and the enzyme-linked immunosorbent assay (ELISA) techniques [31, 32]. The HPLC with UV or mass spectrometric detection is usually exploited for determination and quantification of lysozyme. This method is sensitive and reliable but has some shortcomings such as complexity, time consumption, and high cost for analysis, requiring sample pretreatment and specialized equipment for measurement. The most widely used method for analysis of proteins is ELISA technique which quantifies soluble compounds such as peptides and proteins as well as antibodies. With its high sensitivity and specificity, this method is commonly applied for analysis of various proteins. Nevertheless, ELISA itself still have some limitations such as time-consuming and inability for on-site testing. It is also restrained by the commercially available antibodies with high cost for analysis. Hence, there is still a great need of simple, rapid, on-site testing methodologies for detection of protein biomarkers.

Herein, antilysozyme aptamer, called "artificial antibody," which is easy and low-cost production with little batch-to batch variability and resistance to denaturation and degradation, was exploited to develop a simple, cost-effective, label-free, and ultrasensitive assay for the colorimetric detection of lysozyme. Our design exploits lysozyme-binding aptamer-complementary DNA (cDNA) as a probe and uses AuNPs as a transducer. The transduction principle is based on the electrostatic difference between single-stranded DNA (ssDNA) and double-stranded DNA (dsDNA) upon interaction with *colloidal* gold. Our strategy utilizes the conformational change of dsDNA induced by target and the binding characteristics of DNA aptamer with its target. In the absence of lysozyme, the dsDNA cannot adsorb and stabilize the gold colloid against aggregation when adding high amount of salt. In case of the presence of lysozyme, the dsDNA is dissociated due to the specific interaction between lysozyme and antilysozyme aptamer. This leads to release the cDNA from the duplex structure that helps stabilize the AuNPs, thus protecting them from aggregation upon the high salt concentration. Such an approach allowed the detection of lysozyme at femtomolar level by simple spectroscopic analysis with detection time of ~40 min. In case of naked eye detection, the limit of detection of nanoaptasensor corresponds to ~0.5 pM. The nanoaptasensor also displayed high specificity with regard to lysozyme. Compared with existing method, our sensing approach showed many benefits in terms of simplicity, cost, and time for on-site analysis. This sensing platform not only detects lysozyme but also is applicable to the detection of various biomolecules.

2. Materials and Methods

2.1. Materials. Hydrogen tetrachloroaurate(III) trihydrate ($HAuCl_4.3H_2O$, 99.9%), trisodium citrate, PBS buffer, lysozyme, bovine serum albumin (BSA), trypsin, and α-amylase from human saliva were supplied from Sigma-Aldrich Co., St Louis, MO (USA). Tris(hydroxymethyl)aminomethane (Tris), sodium chloride, hydrochloric acid, and casein were obtained from the Xilong Chemical Co., Ltd. (China). Insulin was purchased from the Eli Lilly Co., Indiana (UK). Trypsin-EDTA 1X was purchased from Gibco (UK). Complementary DNA (5′-CTA AGT AAC TCT GCA CTC TTA TAT ATC ATA GAA TTG GTA GAT-3′) and lysozyme-binding aptamer (5′-ATC TAC GAA TTC ATC AGG GCT AAA GAG TGC AGA GTT ACT TAG-3′) [27] were purchased from Phu Sa Biochem Co. (Vietnam). The simulated saliva samples that contain cationic and ionic ions, amino acids, and α-amylase from human saliva were prepared in the lab [33]. Other reagents and chemicals used in this research were of AR grade. Distilled water (18.2 MΩ cm^{-1}) was used as the solvent to prepare all solutions used in the study.

2.2. Synthesis and Characterization of AuNPs. In this research, citrate-capped AuNPs were synthesized by reducing hydrogen tetrachloroaurate(III) trihydrate with trisodium citrate as described in the previous studies [8, 34]. In brief, hydrogen tetrachloroaurate(III) trihydrate (1.0 mM, 10 mL) was added to a clean bottle and heated to boiling. Subsequently, sodium citrate (1%, 1 mL) was added to the boiling solution while agitating vigorously. This leads to the formation of the monodisperse spherical AuNPs with diameter of ~14 nm. The solution was boiled for 5 minutes to complete the citrate reduction of the tetrachloroaurate(III) ions. The resulting solution was cooled down to room temperature and filtered for removing aggregated nanoparticles. The nanoparticle size and shape were characterized by microplate reader (Varioskan™, Thermo Scientific, USA) and high-resolution transmission electron microscopy on a JEM3010 instrument. Size distribution of AuNPs was analyzed by Zetasizer Nano ZS (Malvern Instruments).

2.3. Preparation of dsDNA. The complementary DNA (cDNA) was hybridized with lysozyme-binding aptamer by mixing the aptamer (100 μM, 1 μL) with cDNA (100 μM, 1 μL), followed by addition of 8 μL annealing buffer that contains 10 mM Tris-HCl (pH 7.5), 50 mM NaCl, and 1 mM EDTA. The resulting solution was heated to 90°C for 5 min, the solution temperature was slowly lowered from 90°C to 60°C for 30 min, and the temperature of solution was then slowly decreased to 4°C to give dsDNA solution. The result of DNA hybridization will be verified by gel electrophoresis.

2.4. Investigation of Electrostatic Property of ssDNA and dsDNA. In this study, the electrostatic difference between ssDNA and dsDNA was exploited to develop the nanoparticle-based colorimetric biosensor. Therefore, it is needed to verify the feasibility of this sensing approach. Firstly, AuNPs (100 μL, 10 nM) was mixed with the ssDNA aptamer/dsDNA (5 μL, 10 μM). Subsequently, the mixture was kept at room temperature for 20 min to allow the DNA to cover completely the nanoparticles surface. Then NaCl (1 M, 10 μL) was rapidly added to the mixture above. The difference in electrostatic properties of ssDNA with dsDNA when interacting with colloidal nanoparticles upon exposure to a high electrolytic environment was recorded by visual inspection and UV-Vis absorption spectrophotometry.

2.5. Effect of Salt Concentration on Aggregation of AuNPs in the Presence of dsDNA. Sodium chloride is an important element that has the influence on the stability of nanoparticles and the sensitivity of the assay. Hence, before conducting the colorimetric assays for lysozyme analysis, it is needed to determine a minimum amount of salt to aggregate completely AuNPs in the presence of dsDNA. Firstly, gold colloid (10 nM, 100 μL) was mixed with dsDNA (10 μM, 5 μL). Next, various amount of 1 M solution of salt was added to the mixture with the final salt concentrations ranging from 0 to 0.12 M. The stability of dsDNA-AuNPs was observed by the unaided eye and UV-Vis absorption spectrophotometry. The minimum amount of salt which induces the complete aggregation of dsDNA-AuNPs was chosen for colorimetric detection of lysozyme.

2.6. Colorimetric Assay for Detection of Lysozyme. To perform the colorimetric assays for detection of lysozyme, 5 μL of the prepared dsDNA was added into a solution containing 10 μL of various concentrations of lysozyme ranging from 0 to 500 pM and incubated at room temperature for 20 min. Next, the mixture was mixed with 100 μL of citrate-capped AuNPs, incubated for 15 min at room temperature. Then the appropriate amount of 1 M NaCl was quickly added to the mixture. After incubation for 5 min, the solution was analyzed by naked eyes and UV-Vis absorption spectrophotometry (Varioskan™, Thermo Scientific, USA). The UV-Vis absorption spectrum was recorded from 400 nm to 800 nm, and the ratio of A620/A520 was used for quantitative analysis. All the data were collected from at least three independent measurements.

2.7. Nonspecific Binding Assays. To ensure the biosensor response due to the specific interaction between DNA aptamer and lysozyme, the sensing platform was challenged by measuring the response of sensor to the nonspecific proteins such as casein, insulin, and trypsin and bovine serum albumin at concentration which was higher than the saturation response concentration of aptasensor. All reaction conditions were kept unchanged as in case of the detection of lysozyme.

3. Results and Discussion

In this study, the target-induced aggregation of AuNPs upon salt addition leading to changes in the color and the UV-Vis spectrum of colloidal solution was exploited for lysozyme sensing. The sensing mechanism of the proposed method is demonstrated in Scheme 1. As shown in the scheme, DNA aptamer was utilized as a specific biorecognition element in colorimetric sensor, and the AuNPs was exploited

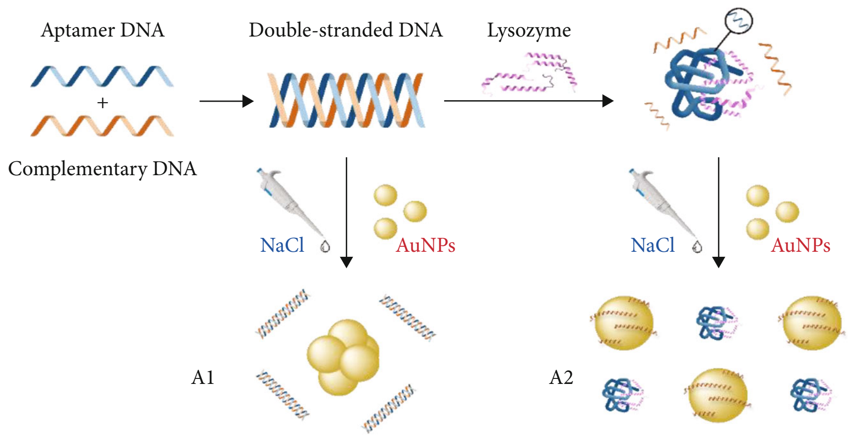

Scheme 1: Experimental scheme illustrating the experimental processes. (a1) In the absence of lysozyme, the color of solution changes from red to blue. (a2) In the presence of lysozyme, the colloidal solution keeps red in color.

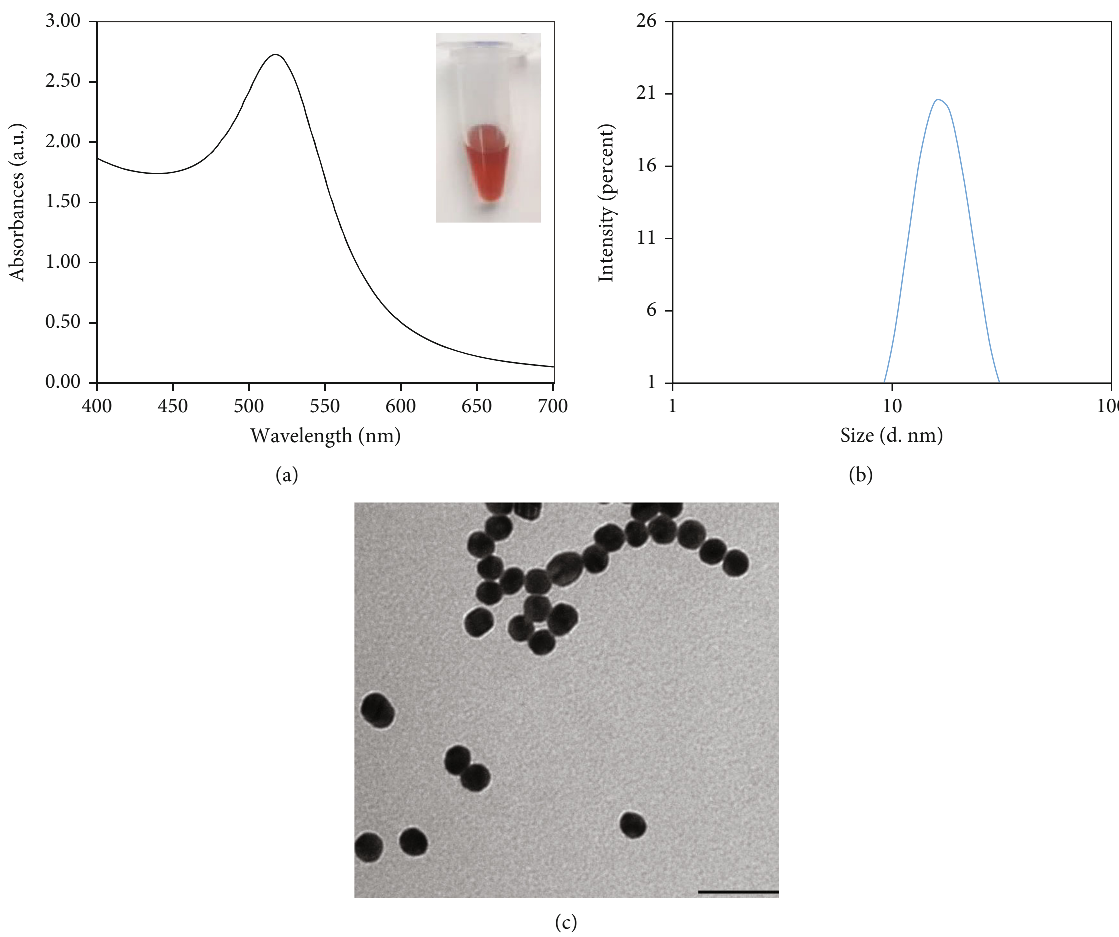

Figure 1: Characterization of AuNPs. (a) The UV–Vis absorbance spectrum of AuNPs; (b) size distribution of AuNPs measured by *Zetasizer Nano* ZS (*Malvern* Instruments); (c) morphology and size of AuNPs with diameter of ~14 nm (TEM).

as a signal transducer to sense the interaction between DNA aptamer and lysozyme. In this case, the functionality of sensor is related to changes in the colloidal stability of gold nanoparticles upon target binding, and the target recognition that causes the changes in surface plasmon resonance of AuNPs leads to color changes that are visible to the naked eye [35]. The sensor was designed based on the difference in electrostatic properties between ssDNA and dsDNA when interacting with AuNPs in solution. It is well known that the key difference between ssDNA and dsDNA relates to the flexibility of their molecular structure. ssDNA is much more flexible compared to dsDNA, and hence, it is able to stabilize the noble metal nanoparticles against the salt-induced aggregation by adsorbing their nucleobases to the

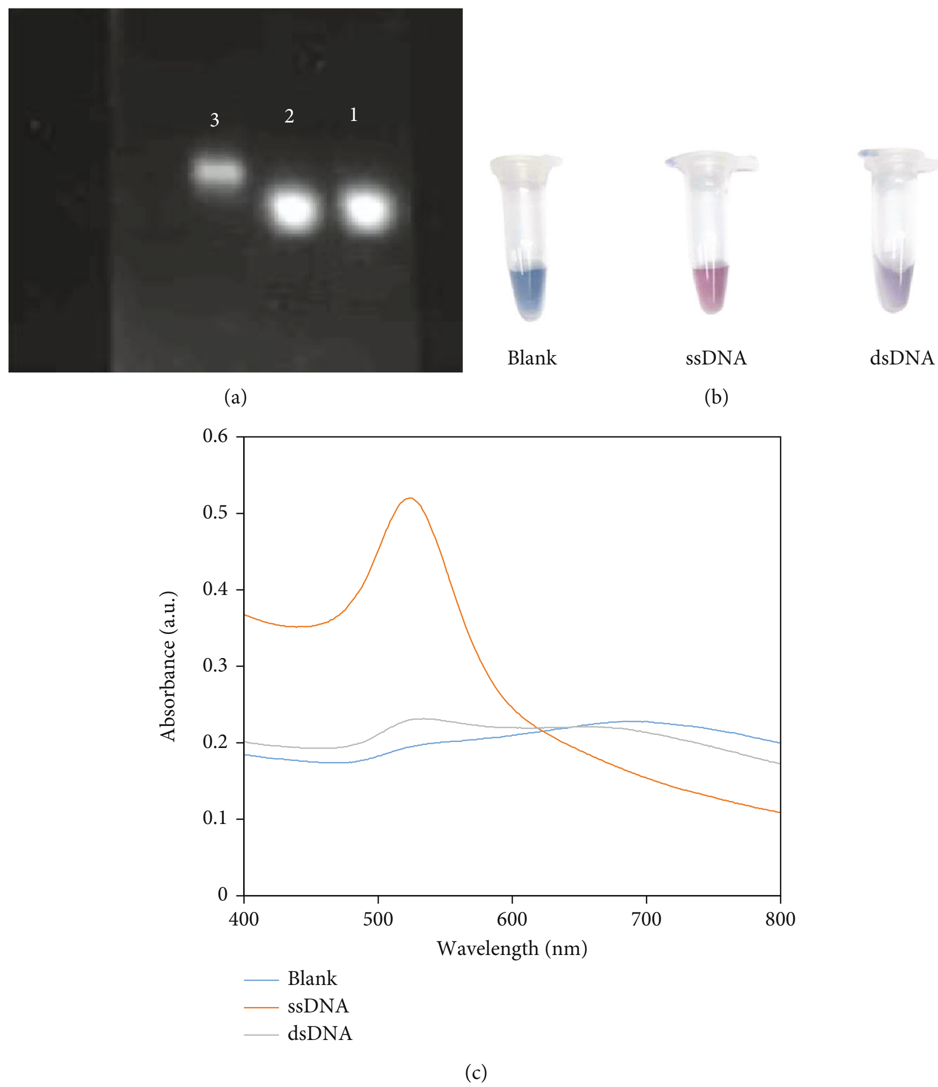

Figure 2: (a) Testing the dsDNA by agarose gel electrophoresis before lysozyme sensing. Lane 1: DNA aptamer (ssDNA); Lane 2: complementary DNA (cDNA); Lane 3: double-stranded DNA (dsDNA); (b) photograph depicting visual color change of AuNPs when interacting with dsDNA and ssDNA upon exposure to a high electrolytic environment; (c) UV-Vis spectrum of respective samples.

nanoparticle surface while exposing the charged phosphate moieties to the solvent [24, 36]. In brief, the interfacial binding features of DNA aptamer with its target, as well as the conformational change of DNA aptamer-complementary DNA (dsDNA) induced by target, were exploited for detection of lysozyme. In the absence of lysozyme, the dsDNA cannot adsorb on the nanoparticle surface to stabilize AuNPs against aggregation upon exposure to a high electrolytic environment. This leads to an obvious color change of gold colloid from ruby red to blue/purple, which can be controlled by visual inspection or spectroscopic analysis. Upon recognition of the lysozyme by DNA aptamer, the affinity of DNA aptamer with its target leads to the detachment of DNA aptamer from the duplex DNA and the release of cDNA molecules. In this case, the cDNA helps to protect the AuNPs from salt-induced aggregation of nanoparticles by electrostatic repulsion. The electrostatic repulsions among adjacent AuNPs owing to negative charge of cDNA keep them dispersed in solution. Moreover, the electrostatic repulsion assists in the prevention of the strong van der Waals attraction, which led to enhance the stability of AuNPs. As a result, the colloidal gold maintains the original ruby red color.

The chemically synthesized AuNPs were first prepared by the reduction of tetrachloroaurate (III) ion with sodium citrate using the Turkevich method [8, 34]. In this method, 1% sodium citrate solution was added to the boiling solution that contains hydrogen tetrachloroaurate (III) while stirring vigorously. This method produced homogeneous spherical AuNPs with average size of ~14 nm as demonstrated in Figure 1. The absorption peak of the ruby red colloid solution occurred at 520 nm and assigned to the localized surface plasmon resonance (LSPR) of AuNPs [8]. The access amount of citrate anion in the reduction reaction gives the nanoparticles a negative charge on the surface, and it helps to stabilize the AuNPs against the aggregation. The concentration of citrate-capped AuNPs was around 10 nM that was determined based on Beer-Lambert law and the average diameter of AuNPs [37, 38]. The dynamic light scattering

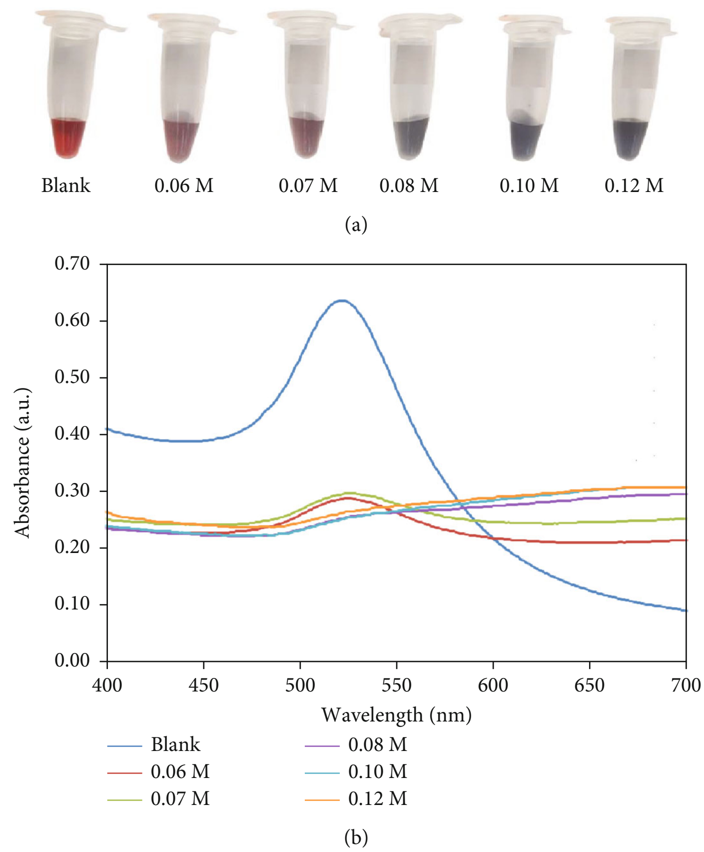

Figure 3: Effect of ionic strength on the plasmon characteristics of the AuNPs in the presence of dsDNA. (a) The color change of colloidal solution of AuNPs at various concentration of salt (0-0.12 M); (b) UV-Vis spectra of respective samples.

(DLS) measurements shows that the average size of the AuNPs was 13.7 ± 1.23 with the polydispersity index (PDI) of 0.148 ± 0.02. With a value of 0.148, it shows that the size of AuNPs is fairly homogenous. The zeta potential of the AuNPs was found at −36.8 mV ± 7.4. It means that AuNPs have a negative charge. The value of zeta potential represents for the stability of the colloidal gold solution. When the zeta potential is high, the solution is more stable, and when the zeta potential is low, the solution is poor stable. Here, the zeta potential of citrate-capped AuNPs is larger than -30 mV; it means that the AuNPs is quite stable.

To test the hybridization between DNA aptamer and cDNA, the aptamer was mixed with cDNA and then incubated at 90°C for 5 min. Afterward, the mixture was slowly decreased to 60°C and incubated for 30 min. The binding of two DNA strands was verified by gel electrophoresis 1% at 100 V. As seen in Figure 2(a), band 1 and band 2 contain ssDNA with equal mass; hence, both bands run in parallel and run faster than band 3 (dsDNA). This indicated that two DNA strands were effectively bound each other. To verify the feasibility of sensing approach, the difference in electrostatic interactions of ssDNA–AuNPs and dsDNA–AuNPs was determined based the selective aggregation of AuNPs with dsDNA in high electrolytic medium. As shown in Figure 2(b), in the presence of ssDNA, the gold colloidal solution keeps its red dispersed state and the resonance peak at 520 nm due to absorption of ssDNA on the nanoparticle's surface, resulted in the protection of the AuNPs against salt-induced aggregation [24, 36]. This adsorption contributes to a charge redistribution that makes the nanoparticle surface appear more negatively charged. Conversely, dsDNA cannot protect the nanoparticle against salt-induced aggregation, and the colloidal solution turns blue/purple. It is well-known that AuNPs are stabilized by negative charge of citrate anions adsorbed on the gold surface. The repulsion between the adsorbed citrate anions and the charged phosphate backbone of dsDNA governs the electrostatic interaction between AuNPs and dsDNA. As a result, dsDNA cannot adsorb on the nanoparticle surface. This difference is due to the fact that ssDNA can unwind adequately to expose its bases on the nanoparticle surface, whereas the DNA duplex has a steady double-helix structure that always shows the negative charge of phosphate backbone [36, 39]. The difference in electrostatic interaction of ssDNA-AuNPs and dsDNA-AuNPs can be exploited to design the colorimetric assay for detection of analytes.

It is noted that the applications of AuNPs are strongly influenced by stable state of nanoparticles in solution, especially for those based on nanoparticle aggregation assays [35]. The AuNPs are extremely stable and well dispersed in aqueous solution due to the negatively charged citrate ions on their surface. Salt is the key element that affects the aggregation of gold colloid. In this study, sodium chloride was used as *aggregating*-ion to sense the release of cDNA from

(a)

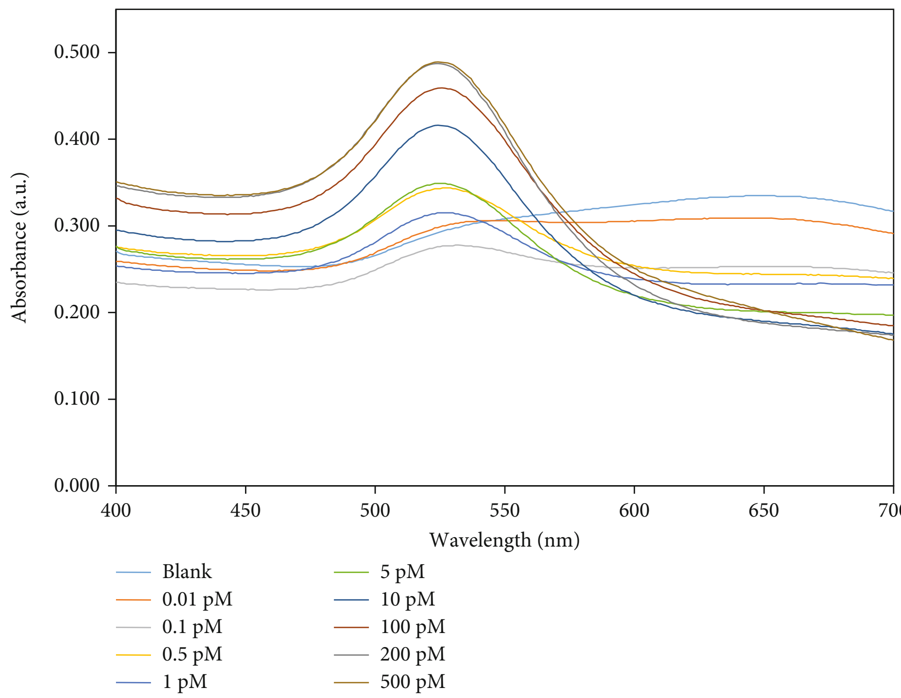

(b)

Figure 4: Colorimetric nanoaptasensor for analysis of lysozyme based on the electrostatic interaction of ssDNA-AuNPs and dsDNA-AuNPs. (a) The color response of dsDNA-AuNPs as a function of lysozyme concentration after salt addition; (b) UV–Vis absorption spectra of dsDNA-AuNPs in the presence of various concentration of lysozyme from 0.01 to 500 pM.

the dsDNA. Hence, the concentration of salt in the solution directly affects the sensitivity of the sensor. To determine an optimal ratio of salt to AuNPs, the nanoparticle *aggregation* was tested at various concentrations of *salt* in the presence of dsDNA. Figure 3 shows the effect of ionic strength on the plasmon characteristics of the AuNPs in the presence of dsDNA. As demonstrated in Figure 3(a), the color of gold colloid turned from ruby red to purple/blue upon increasing concentration of salt, denoting the changes in surface charge of AuNPs that led to their aggregation [40, 41]. This observation was further supported by the UV-Vis absorption spectra of gold colloid. As shown in Figure 3(b), the UV-Vis absorption spectra revealed a sharp decrease in the absorbance peak at 520 nm, and the absorbance additionally decreased upon increasing salt amount in the colloidal solution. It reached a plateau as the concentration of NaCl was at 0.08 M or higher than that owing to the complete aggregation of nanoparticles. Moreover, as the result of increasing salt concentration, a second resonant peak at a longer wavelength around 620 nm emerged on account of the formation of blue/purple colored aggregates. In this case, the lowest concentration of salt that induces the complete aggregation of AuNPs was 0.08 M. Hence, this concentration was chosen for the following experiments.

For lysozyme analysis, numerous concentrations of lysozyme from 0 to 500 pM were mixed with dsDNA-AuNPs, followed by the addition of salt with final concentration of 0.08 M, and the color alteration and spectroscopic response were analyzed. As shown in Figure 4, with the presence of lysozyme, the specific interaction between lysozyme and the DNA aptamer against lysozyme resulted in the dissociation of the aptamer from the dsDNA and forms a structured complex. In addition, the cDNA molecule detached from the DNA duplex adsorbed on the nanoparticle surface worked as a shield against salt-induced aggregation of nanoparticles, resulted in maintaining the dispersed state of AuNPs and the typical resonance peak at 520 nm. Conversely, in the absence or very low concentration of lysozyme, the color of gold colloids changed to blue/purple, and the UV-Vis absorption spectra of AuNPs exhibited a significant reduction in the absorbance peak at 520 nm as well as a peak at ~620 nm emerged owing to the redshift of the resonance peak, resulted from the formation of gold nanoaggregates. In this case, the AuNPs were not protected due to the absence of

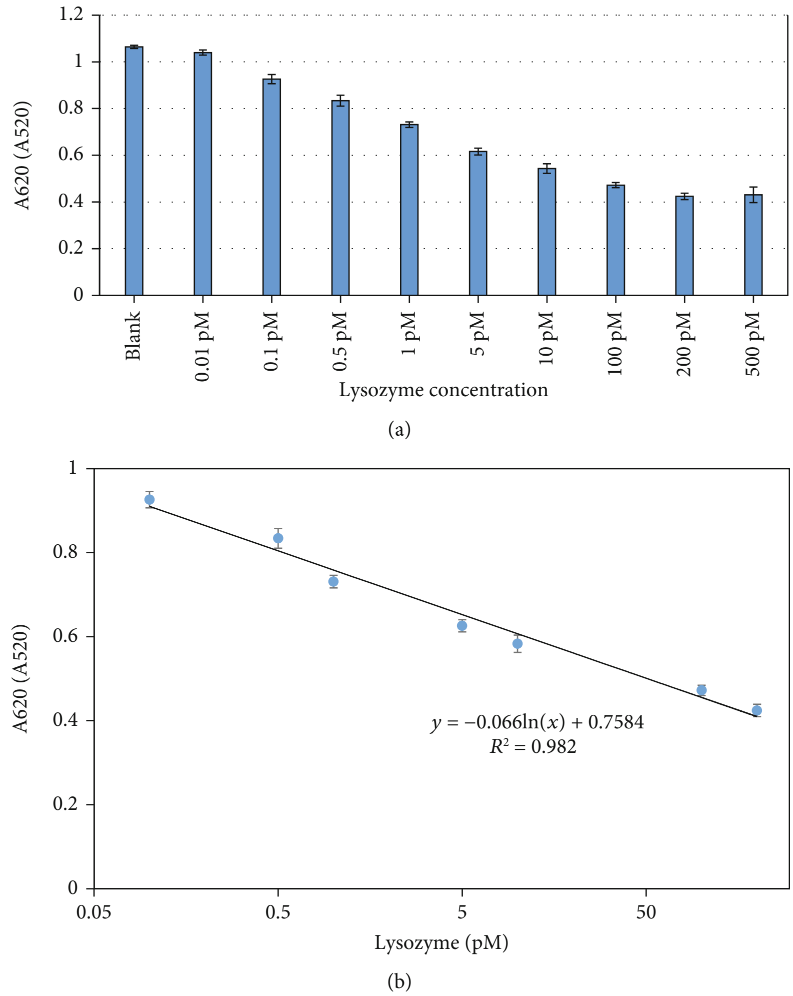

Figure 5: (a) The response of absorbance ratio (A620/A520) for the various concentrations of lysozyme from 0 to 500 pM. (b) The linear calibration curve depicting the relation between lysozyme concentrations and absorbance ratio (A620/A520).

a *cDNA* and nonabsorption of dsDNA on the nanoparticle surface. With the increase of lysozyme concentration from 0 to 500 pM, the color of solution gradually changed from blue to red color, the resonance peak at 520 nm increased, while the peak around 620 nm decreased gradually which indicated the well-dispersed state of nanoparticles. In Figure 4, it is easy to realize that the lysozyme concentration of ~0.5 pM is the concentration that can be detected with the naked eye. The investigation of UV-Vis absorption spectroscopy of dsDNA-AuNPs also revealed that the absorbance ratio (A620/A520) is proportional to the concentration of lysozyme. Hence, this absorbance ratio was used to evaluate the sensitivity of assay and the stability of AuNPs that were induced by the presence of lysozyme. In other words, the sensitivity of proposed assay was calculated by controlling the change of the ratio (A620/A520) after addition of the various concentrations of lysozyme. Moreover, by calculating the ratio (A620/A520) via the UV-Vis measurement, we could measure the concentration of lysozyme, which is crucial for quantitative analysis of lysozyme.

Figure 5 shows the linear scale between the absorbance ratio (A620/A520) and lysozyme concentration. The negative linear regression equation for lysozyme detection with linear range from 0.1 to 200 pM was $y = -0.066\ \ln(x) + 0.7584$ with $R^2 = 0.982$, where x and y are lysozyme concentration (pM) and the absorbance ratio of A620/A520, respectively. Based on the linear regression equation obtained from Figure 5, the concentration of lysozyme in samples could be determined. The limit of detection (LOD) of the proposed assay can be calculated through the measurement of the standard deviation of blank sample (α) and the slope of the linear regression equation (s) according to the formula $3\alpha/s$. The lowest concentration of the lysozyme could be determined as low as 0.05 pM (~50 fM).

It is essential to test the nonspecific binding between nontarget proteins and antilysozyme aptamer to verify the observed change of the absorbance ratio (A620/A520) owing to the specific interaction between lysozyme and antilysozyme aptamer and to confirm the limit of detection of nanoaptasensor. That is because unexpected interaction events can produce false signal in the quantitative analysis. In this study, the specificity test was carried out on a series of interfering proteins in human fluids at concentration of 10 nM, which was much higher than that of the saturation response of nanoaptasensor. These proteins have different molecular weights and isoelectric points, and they are very

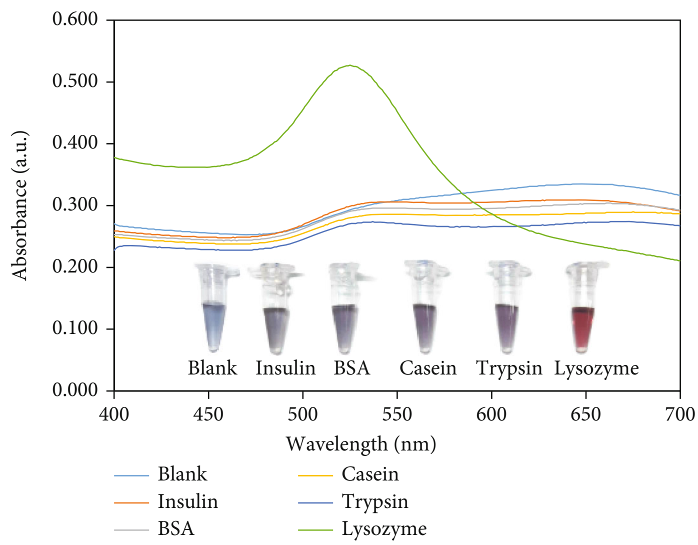

(a)

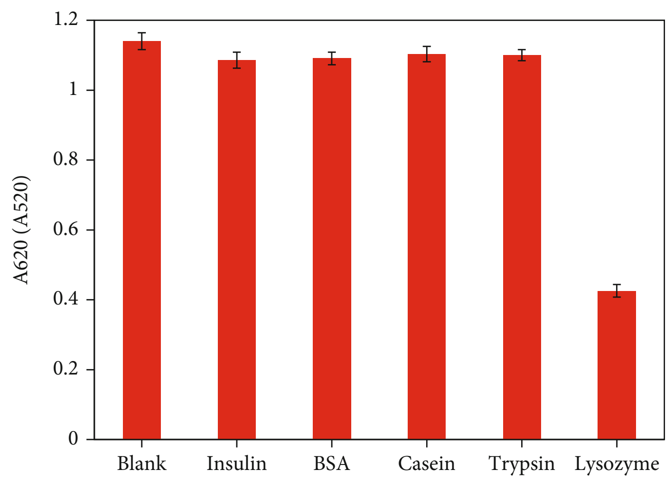

(b)

Figure 6: Nonspecific binding of different interfering proteins with concentration of 10 nM on the nanoaptasensor's surface compared to the specific binding of lysozyme with concentration of 500 pM. (a) The UV/Vis spectra and color response of designed assay to lysozyme in comparison with other proteins; (b) specificity of designed assay in the presence of different proteins.

common proteins in human fluids at high concentrations, having opposite net charges, which have been studied on a variety of other studies [8, 42, 43]. Hence, they are ideal for the study of nonspecific interaction induced by electrostatic interactions. From the visual inspection results in Figure 6, it clearly indicated that only the specific binding between lysozyme and antilysozyme aptamer can prevent the formation of blue/purple aggregates from the ruby red dispersed state of AuNPs in the presence of high concentration of salt. As clearly demonstrated in Figure 6, the absorbance ratio (A620/A520) upon the presence of lysozyme was much smaller than that of the interfering proteins. Compared to the change of the absorbance ratio from the specific binding of lysozyme with antilysozyme aptamer, which were tested in a concentration range of 0.01 to 500 pM, these changes were negligible. These results confirm that the proposed assay for lysozyme analysis is very highly specific, and it could be exploited for the detection of lysozyme with ultrahigh sensitivity. The femtomolar sensitivity of the proposed assay is large enough to detect lysozyme available in human body fluids and food [44]. The detection limit and linear dynamic range we obtained in this study provided an improved analytical performance compared with other types of colorimetric assays and biosensors that have been applied to detection and quantification of lysozyme as described in Table 1. The analytical performance of this assay can compare with the values obtained from the assays based on the electrochemical impedance spectroscopy that exploited the electrodeposited AuNPs [45] and droplet-based microfluidic devices that utilized the aptamer-modified AuNPs-enhanced chemiluminescence [46]. Specifically, it was much lower than those achieved with the assays based on electrostatic interaction with albumin-modified AuNPs (LOD = 50 nM) [47], with fluorescent aptasensor using magnetic separation (LOD = 0.2 nM) [48], with electrochemical aptasensor using signal-off architecture (0.45 nM) [49],

Table 1: Comparison of proposed nanoaptasensor with other types of colorimetric assays and biosensors applied to lysozyme detection.

Assay formats and/or biosensor formats	Linear dynamic range	Detection limit	References
Assay based on electrostatic interaction with human serum albumin-modified AuNPs	18.7–561 nM	50 nM	[47]
Fluorescent aptasensor based on magnetic separation	0.56–12.3 nM	0.2 nM	[48]
Electrochemical impedance spectroscopy aptasensor based on electrodeposited AuNPs	0.1–500 pM	0.01 pM	[45]
Assay based on resonant Rayleigh scattering spectroscopy	7×10^2–7×10^5 aM	7 aM	[8]
Signal-off architecture for electrochemical aptasensor	7–30 nM	0.45 nM	[49]
Aptasensor based on electron transfer	1–80 nM	0.5 nM	[26]
Digital microfluidic-based assay	40 fM-300 fM	44.6 fM	[46]
Electrochemical aptasensor utilizing target-induced turn-off of photosensitization	0.01-100 nM	2 pM	[27]
Assay based on capillary electrophoresis and inductively coupled plasma mass spectrometry	0–41.4 fM	3.89 aM	[51]
Nanoaptasensor based on electrostatic interaction of ssDNA-AuNPs and dsDNA-AuNPs	0.1–200 pM	50 fM	Our work

with aptasensor based on electron transfer (LOD = 0.5 nM) [26], and with the electrochemical aptasensor that exploited the lysozyme-induced turn-off of photosensitization (LOD = 2 pM) [27]. Compared to the LOD of commercially available ELISA kits for lysozyme analysis (LOD~2.72 pM) [50], our proposed approach achieved much lower LOD. The detection platform we described could compete with standard ELISA assays for proteins analysis. It helps to overcome limitations that affect ELISA assays such as analysis time, narrow dynamic range, and the cross-reactivity of detection antibodies that are responsible for producing nonspecific response of assays. The sensing platform based on the difference in electrostatic interaction of ssDNA-AuNPs and dsDNA-AuNPs is ultrasensitive for analysis of protein biomarkers, and it has great potential for early detection of diseases. However, its detection limit was still higher than that of our previous study upon the resonant Rayleigh scattering spectroscopy of single nanoparticle [8] and the assay based on capillary electrophoresis and inductively coupled plasma mass spectrometry [51]. Compared with the available analytical methods and other types of biosensors applied to lysozyme detection that require sample pretreatment, time consumption, high cost for analysis, complexity, requiring specialized equipment for measurement, and inability for on-site testing, this proposed nanoaptasensor shows its convenience with regard to simplicity, versatility, low experimental cost, short time for analysis, and ability for point of care testing of target proteins.

To assess the feasibility of proposed platform for possible application in real samples, the simulated saliva samples that contain cationic and ionic ions, amino acids, and α-amylase from human saliva were tested. Three simulated saliva samples spiked with 10 pM, 100 pM, and 150 pM of lysozyme were analyzed by proposed nanoaptasensor. As shown in Table 2, the satisfactory recoveries were ranging from 90.47 to 105.90%, and the relative standard deviations (RSD) were below 5% (3.45-4.89%) that suggests a good reproducibility. The results clearly indicated the reliability and applicability of the proposed method for the simple and rapid detection of lysozyme in real samples.

Table 2: Lysozyme recovery in simulated saliva samples.

Spiked concentration (pM)	Found concentration (pM)	Recovery (%)	RSD (%)
10.00	9.58	95.80	3.45
100.00	90.47	90.47	4.89
150.00	158.86	105.90	4.21

4. Conclusions

We have demonstrated a simple, fast, cost-effective, and ultrasensitive nanoaptasensor for colorimetric detection of proteins based on the target-induced conformational change of DNA duplex. The detection method utilizes the interaction between DNA aptamer and its target leading to the dissociation of DNA aptamer from the DNA duplex and forms a structured complex, and the cDNA that released from the DNA duplex adsorbed on the AuNPs surface protects the nanoparticle against salt-induced aggregation, resulted in keeping the red dispersed state of AuNPs. This nanoaptasensor is suitable for point-of-care detection of protein biomarkers due to the rapid salt induced aggregation of AuNPs and easy to recognize the change in color of colloidal gold and state of the resultant solution. Using lysozyme and antilysozyme aptamer as a model for detection of proteins, the proposed nanoaptasensor could detect as low as 50 fM with a wide linear dynamic range from 0.1 to 200 pM. The most important feature of this approach is the direct detection of lysozyme by unaided eye or *simple*, *low-cost absorbance* measurement device. Owing to the simplicity and versatility of the developed nanoaptasensor, it can be an alternative diagnostic assay for determination and quantification of not only lysozyme but also other protein biomarkers.

Data Availability

The authors confirm that the data supporting the findings of this study are available within the article [and/or] its supplementary materials.

Conflicts of Interest

The authors have no conflicts of interest.

Acknowledgments

This research is funded by International University, VNU-HCM under grant number T2019-01-BME.

References

[1] E. V. Campos, A. E. Pereira, J. L. De Oliveira et al., "How can nanotechnology help to combat COVID-19? Opportunities and urgent need," *Journal of Nanobiotechnology*, vol. 18, no. 1, pp. 125–223, 2020.

[2] H. Malekzad, P. S. Zangabad, H. Mirshekari, M. Karimi, and M. R. Hamblin, "Noble metal nanoparticles in biosensors: recent studies and applications," *Nanotechnology Reviews*, vol. 6, no. 3, pp. 301–329, 2017.

[3] H. Aldewachi, T. Chalati, M. N. Woodroofe, N. Bricklebank, B. Sharrack, and P. Gardiner, "Gold nanoparticle-based colorimetric biosensors," *Nanoscale*, vol. 10, no. 1, pp. 18–33, 2018.

[4] J. Zhuang, W. Lai, M. Xu, Q. Zhou, and D. Tang, "Plasmonic AuNP/g-C3N4 nanohybrid-based photoelectrochemical sensing platform for ultrasensitive monitoring of polynucleotide kinase activity accompanying DNAzyme-catalyzed precipitation amplification," *ACS Applied Materials & Interfaces*, vol. 7, no. 15, pp. 8330–8338, 2015.

[5] J. Shu, Z. Qiu, S. Lv, K. Zhang, and D. Tang, "Plasmonic enhancement coupling with defect-engineered TiO2−x: a mode for sensitive photoelectrochemical biosensing," *Analytical Chemistry*, vol. 90, no. 4, pp. 2425–2429, 2018.

[6] G. Cai, Z. Yu, R. Ren, and D. Tang, "Exciton–plasmon interaction between AuNPs/graphene nanohybrids and CdS quantum Dots/TiO2 for photoelectrochemical aptasensing of prostate-specific antigen," *ACS sensors*, vol. 3, no. 3, pp. 632–639, 2018.

[7] J. N. Anker, W. P. Hall, O. Lyandres, N. C. Shah, J. Zhao, and R. P. Van Duyne, "Biosensing with plasmonic nanosensors," *Nature Mater*, vol. 7, no. 6, pp. 442–453, 2008.

[8] P. L. Truong, S. P. Choi, and S. J. Sim, "Amplification of resonant Rayleigh light scattering response using immunogold colloids for detection of lysozyme," *Small*, vol. 9, no. 20, pp. 3485–3492, 2013.

[9] J. S. Lee, A. K. Lytton-Jean, S. J. Hurst, and C. A. Mirkin, "Silver nanoparticle-oligonucleotide conjugates based on DNA with triple cyclic disulfide moieties," *Nano Letters*, vol. 7, no. 7, pp. 2112–2115, 2007.

[10] A. D. McFarland and R. P. Van Duyne, "Single silver nanoparticles as real-time optical sensors with zeptomole sensitivity," *Nano Letters*, vol. 3, no. 8, pp. 1057–1062, 2003.

[11] R. Ren, G. Cai, Z. Yu, Y. Zeng, and D. Tang, "Metal-polydopamine framework: an innovative signal-generation tag for colorimetric immunoassay," *Analytical Chemistry*, vol. 90, no. 18, pp. 11099–11105, 2018.

[12] Z. Gao, Z. Qiu, M. Lu, J. Shu, and D. Tang, "Hybridization chain reaction-based colorimetric aptasensor of adenosine 5′-triphosphate on unmodified gold nanoparticles and two label-free hairpin probes," *Biosensors and Bioelectronics*, vol. 89, Part 2, pp. 1006–1012, 2017.

[13] Z. Gao, M. Xu, L. Hou, G. Chen, and D. Tang, "Magnetic bead-based reverse colorimetric immunoassay strategy for sensing biomolecules," *Analytical Chemistry*, vol. 85, no. 14, pp. 6945–6952, 2013.

[14] H. Jans and Q. Huo, "Gold nanoparticle-enabled biological and chemical detection and analysis," *Chemical Society Reviews*, vol. 41, no. 7, pp. 2849–2866, 2012.

[15] C. McVey, F. Huang, C. Elliott, and C. Cao, "Endonuclease controlled aggregation of gold nanoparticles for the ultrasensitive detection of pathogenic bacterial DNA," *Biosensors and Bioelectronics*, vol. 92, pp. 502–508, 2017.

[16] M. Holzinger, A. Le Goff, and S. Cosnier, "Nanomaterials for biosensing applications: a review," *Frontiers in Chemistry*, vol. 2, p. 63, 2014.

[17] P. L. Truong, X. Ma, and S. J. Sim, "Resonant Rayleigh light scattering of single Au nanoparticles with different sizes and shapes," *Nanoscale*, vol. 6, no. 4, pp. 2307–2315, 2014.

[18] X. Zhao, H. Zhao, L. Yan, N. Li, J. Shi, and C. Jiang, "Recent developments in detection using noble metal nanoparticles," *Critical Reviews in Analytical Chemistry*, vol. 50, no. 2, pp. 97–110, 2020.

[19] M. Cárdenas, J. Barauskas, K. Schillén, J. L. Brennan, M. Brust, and T. Nylander, "Thiol-specific and nonspecific interactions between DNA and gold nanoparticles," *Langmuir*, vol. 22, no. 7, pp. 3294–3299, 2006.

[20] L. Shen, P. Wang, and Y. Ke, "DNA nanotechnology-based biosensors and therapeutics," *Advanced Healthcare Materials*, vol. 10, no. 15, p. 2002205, 2021.

[21] M. Sabela, S. Balme, M. Bechelany, J. M. Janot, and K. Bisetty, "A review of gold and silver nanoparticle-based colorimetric sensing assays," *Advanced Engineering Materials*, vol. 19, no. 12, p. 1700270, 2017.

[22] N. Kasyanenko, M. Varshavskii, E. Ikonnikov et al., "DNA modified with metal nanoparticles: preparation and characterization of ordered metal-DNA nanostructures in a solution and on a substrate," *Journal of Nanomaterials*, vol. 2016, 12 pages, 2016.

[23] N. Farkhari, S. Abbasian, A. Moshaii, and M. Nikkhah, "Mechanism of adsorption of single and double stranded DNA on gold and silver nanoparticles: investigating some important parameters in bio-sensing applications," *Colloids and Surfaces B: Biointerfaces*, vol. 148, pp. 657–664, 2016.

[24] H. Li and L. Rothberg, "Colorimetric detection of DNA sequences based on electrostatic interactions with unmodified gold nanoparticles," *Proceedings of the National Academy of Sciences*, vol. 101, no. 39, pp. 14036–14039, 2004.

[25] W. Zhao, M. A. Brook, and Y. Li, "Design of gold nanoparticle-based colorimetric biosensing assays," *Chembiochem*, vol. 9, no. 15, pp. 2363–2371, 2008.

[26] Y. Lian, F. He, X. Mi, F. Tong, and X. Shi, "Lysozyme aptamer biosensor based on electron transfer from SWCNTs to SPQC-IDE," *Sensors and Actuators B: Chemical*, vol. 199, pp. 377–383, 2014.

[27] Z. Chen, Q. Xu, G. Tang, S. Liu, S. Xu, and X. Zhang, "A facile electrochemical aptasensor for lysozyme detection based on target-induced turn-off of photosensitization," *Biosensors and Bioelectronics*, vol. 126, pp. 412–417, 2019.

[28] S. Bamrungsap, M. I. Shukoor, T. Chen, K. Sefah, and W. Tan, "Detection of lysozyme magnetic relaxation switches based on aptamer-functionalized superparamagnetic nanoparticles," *Analytical Chemistry*, vol. 83, no. 20, pp. 7795–7799, 2011.

[29] V. B. Abdul-Salam, P. Ramrakha, U. Krishnan et al., "Identification and assessment of plasma lysozyme as a putative

biomarker of atherosclerosis," *Arteriosclerosis, thrombosis, and vascular biology*, vol. 30, no. 5, pp. 1027–1033, 2010.

[30] S. Ghosh, N. I. Khan, J. G. Tsavalas, and E. Song, "Selective detection of lysozyme biomarker utilizing large area chemical vapor deposition-grown graphene-based field-effect transistor," *Frontiers in Bioengineering and Biotechnology*, vol. 6, p. 29, 2018.

[31] N. Schneider, C. M. Becker, and M. Pischetsrieder, "Analysis of lysozyme in cheese by immunocapture mass spectrometry," *Journal of Chromatography B*, vol. 878, no. 2, pp. 201–206, 2010.

[32] N. Schneider, I. Weigel, K. Werkmeister, and M. Pischetsrieder, "Development and validation of an enzyme-linked immunosorbent assay (ELISA) for quantification of lysozyme in cheese," *Journal of Agricultural and Food Chemistry*, vol. 58, no. 1, pp. 76–81, 2010.

[33] X. Wang, Y. Xu, Y. Chen, L. Li, F. Liu, and N. Li, "The gold-nanoparticle-based surface plasmon resonance light scattering and visual DNA aptasensor for lysozyme," *Analytical and Bioanalytical Chemistry*, vol. 400, no. 7, pp. 2085–2091, 2011.

[34] J. Turkevich, P. C. Stevenson, and J. Hillier, "A study of the nucleation and growth processes in the synthesis of colloidal gold," *Discussions of the Faraday Society*, vol. 11, pp. 55–75, 1951.

[35] Y. S. Kim, N. H. A. Raston, and M. B. Gu, "Aptamer-based nanobiosensors," *Biosensors and Bioelectronics*, vol. 76, pp. 2–19, 2016.

[36] P. A. Mirau, J. E. Smith, J. L. Chávez, J. A. Hagen, N. Kelley-Loughnane, and R. Naik, "Structured DNA aptamer interactions with gold nanoparticles," *Langmuir*, vol. 34, no. 5, pp. 2139–2146, 2018.

[37] X. Liu, M. Atwater, J. Wang, and Q. Huo, "Extinction coefficient of gold nanoparticles with different sizes and different capping ligands," *Colloids and Surfaces B: Biointerfaces*, vol. 58, no. 1, pp. 3–7, 2007.

[38] P. L. Truong, V. T. C. Duyen, and V. V. Toi, "Rapid detection of tebuconazole based on aptasensor and aggregation of silver nanoparticles," *Journal of Nanomaterials*, vol. 2021, Article ID 5532477, 10 pages, 2021.

[39] K. Sato, K. Hosokawa, and M. Maeda, "Rapid aggregation of gold nanoparticles induced by non-cross-linking DNA hybridization," *Journal of the American Chemical Society*, vol. 125, no. 27, pp. 8102-8103, 2003.

[40] R. Pamies, J. G. H. Cifre, V. F. Espín, M. Collado-González, F. G. D. Baños, and J. G. de la Torre, "Aggregation behaviour of gold nanoparticles in saline aqueous media," *Journal of Nanoparticle Research*, vol. 16, pp. 1–11, 2014.

[41] S. C. Gopinath, T. Lakshmipriya, and K. Awazu, "Colorimetric detection of controlled assembly and disassembly of aptamers on unmodified gold nanoparticles," *Biosensors and Bioelectronics*, vol. 51, pp. 115–123, 2014.

[42] V. Silin, H. Weetall, and D. J. Vanderah, "SPR studies of the nonspecific adsorption kinetics of human IgG and BSA on gold surfaces modified by self-assembled monolayers (SAMs)," *Journal of Colloid and Interface Science*, vol. 185, no. 1, pp. 94–103, 1997.

[43] R. J. Green, M. C. Davies, C. J. Roberts, and S. J. B. Tendler, "Competitive protein adsorption as observed by surface plasmon resonance," *Biomaterials*, vol. 20, no. 4, pp. 385–391, 1999.

[44] A. Vasilescu, Q. Wang, M. Li, R. Boukherroub, and S. Szunerits, "Aptamer-based electrochemical sensing of lysozyme," *Chem*, vol. 4, p. 10, 2016.

[45] Z. Chen, L. Li, H. Zhao, L. Guo, and X. Mu, "Electrochemical impedance spectroscopy detection of lysozyme based on electrodeposited gold nanoparticles," *Talanta*, vol. 83, no. 5, pp. 1501–1506, 2011.

[46] M. C. Giuffrida, G. Cigliana, and G. Spoto, "Ultrasensitive detection of lysozyme in droplet-based microfluidic devices," *Biosensors and Bioelectronics*, vol. 104, pp. 8–14, 2018.

[47] Y. M. Chen, C. J. Yu, T. L. Cheng, and W. L. Tseng, "Colorimetric detection of lysozyme based on electrostatic interaction with human serum albumin-modified gold nanoparticles," *Langmuir*, vol. 24, no. 7, pp. 3654–3660, 2008.

[48] L. Wang, L. Li, Y. Xu, G. Cheng, P. He, and Y. Fang, "Simultaneously fluorescence detecting thrombin and lysozyme based on magnetic nanoparticle condensation," *Talanta*, vol. 79, no. 3, pp. 557–561, 2009.

[49] Z. Chen and J. Guo, "A reagentless signal-off architecture for electrochemical aptasensor for the detection of lysozyme," *Electrochimica Acta*, vol. 111, pp. 916–920, 2013.

[50] https://www.abcam.com/human-lysozyme-elisa-kit-lzm-ab108880.html.

[51] M. Yang, W. Wu, Y. Ruan et al., "Ultra-sensitive quantification of lysozyme based on element chelate labeling and capillary electrophoresis–inductively coupled plasma mass spectrometry," *Analytica Chimica Acta*, vol. 812, pp. 12–17, 2014.